Electronic Supplementary Information

Copper(I) complexes with quinolone appended 1,8-naphthalimide conjugates: structural characterization, DNA and protein binding and cytotoxicity studies

Sabiha A. Shaikh[a], Satish S. Bhat[a], Vidyanand K. Revankar*[a], Naveen S.[b], Karthik Kumara[c], N.K. Lokhanath[d], Ray J. Butcher[e], Vijay Kumbar[f] and Kishore Bhat[f]

[a]Department of Chemistry, Karnatak University, Dharwad-580003, Karnataka, India.

[b] Department of Physics, Faculty of Engineering & Technology, Jain (Deemed-to-be University), Bangalore 562112, India

[c] Department of Physics, BMS College of Engineering, Bangaluru-560017.

[d] Department of Studies in Physics, University of Mysore, Manasagangotri, Mysuru 570006, Karnataka, India

[e]Department of Chemistry, Howard University, Washington, DC 20059, USA.

[f]Maratha Mandal's Central Research Laboratory, Marathamandal Dental College and Research Centre, Belgaum, Karnataka, India.

E-mail: vkrevankar@rediffmail.com

Table S1. Selected bond lengths [Å] and bond angles [°] for **L**.

Bond lengths [Å]		**Bond angles [°]**	
O1—C13	1.2229 (18)	C9—N1—C1	117.33 (12)
O2—C14	1.2138 (18)	C10—N2—C11	116.28 (12)
N1—C9	1.3217 (18)	C13—N3—C14	125.49 (11)
N1—C1	1.3725 (18)	C13—N3—C12	117.72 (12)
N2—C10	1.2663 (19)	C14—N3—C12	116.78 (11)
N2—C11	1.4676 (18)	N1—C1—C2	118.18 (13)
N3—C13	1.3917 (18)	N1—C1—C6	122.66 (13)
N3—C14	1.4069 (18)	N3—C13—C23	116.87 (12)
N3—C12	1.4718 (17)	O2—C14—N3	120.38 (13)
C8—C9	1.426 (2)	O2—C14—C15	123.14 (13)
C11—C12	1.530 (2)	N3—C14—C15	116.48 (12)
C9—C10	1.4825 (19)	N1—C9—C8	124.16 (12)

Table S2. Selected bond lengths [Å] and bond angles [°] for complex **1**.

Bond lengths [Å]		**Bond angles [°]**	
Cu1—N2	2.0365 (19)	N2—Cu1—N5	106.40 (8)
Cu1—N4	2.0256 (17)	N4—Cu1—N2	140.16 (7)
Cu1—N5	2.0491 (19)	N4—Cu1—N5	81.33 (7)
Cu1—N1	2.012 (5)	N1—Cu1—N2	77.68 (19)
		N1—Cu1—N4	127.28 (17)
		N1—Cu1—N5	130.5 (2)

Table S3. Selected hydrogen-bond parameters for complex **1**.

D—H···*A*	*D*—H (Å)	H···*A* (Å)	*D*···*A* (Å)	*D*—H···*A* (°)
C8—H8···O22	0.93	2.50	3.286 (10)	142.9
C10—H10···O22	0.93	2.33	3.145 (9)	146.7
C11—H11A···O3^{i}	0.97	2.44	3.156 (7)	130.2
C11—H11A···O3A^{i}	0.97	2.49	3.146 (10)	124.5
C11—H11B···O1	0.97	2.49	3.033 (3)	115.5
C12—H12B···O12	0.97	2.53	3.289 (5)	135.5
C35—H35B···O3	0.97	2.42	2.970 (6)	115.7
O1WA—H1WA···N11	0.89 (2)	2.46 (4)	3.260 (6)	150 (5)
O1WA—H1WA···O11	0.89 (2)	1.85 (3)	2.714 (7)	165 (6)
O1WA—H1WA···O12	0.89 (2)	2.48 (6)	3.060 (7)	124 (5)
O1WA—H1WB···O2	0.84 (2)	2.63 (5)	3.314 (6)	140 (6)
O1WB—H1WD···O2	0.82 (2)	2.00 (3)	2.810 (15)	172 (8)
O2W—H2WA···O3W	0.83 (2)	2.21 (6)	2.993 (9)	156 (12)
O2W—H2WB···O13^{i}	0.84 (2)	2.55 (9)	3.200 (12)	135 (12)
O3W—H3WA···O22^{i}	0.885 (19)	2.01 (5)	2.719 (13)	136 (6)
O3W—H3WA···O2W	0.885 (19)	2.39 (5)	2.993 (9)	126 (5)
O3W—H3WB···O1	0.827 (19)	2.09 (2)	2.911 (4)	172 (5)

Table S4. Selected bond lengths [Å] and bond angles [°] for complex **2**.

Bond lengths [Å]		**Bond angles [°]**	
Cu1—N6	2.024 (3)	N6—Cu1—N2	139.93 (12)
Cu1—N2	2.032 (3)	N6—Cu1—N1	122.25 (11)
Cu1—N1	2.042 (3)	N2—Cu1—N1	81.71 (12)
Cu1—N5	2.044 (3)	N6—Cu1—N5	81.55 (11)
		N2—Cu1—N5	107.33 (12)
		N1—Cu1—N5	131.31 (12)

Table S5. Selected Bond lengths [Å] and bond angles [°] for complex **3**.

Cu1—N2	2.023 (3)	N2—Cu1—N4	135.00 (14)
Cu1—N4	2.034 (3)	N2—Cu1—N1	81.61 (13)
Cu1—N1	2.050 (3)	N4—Cu1—N1	121.55 (12)
Cu1—N5	2.050 (3)	N2—Cu1—N5	106.28 (13)
		N4—Cu1—N5	81.39 (13)
		N1—Cu1—N5	139.25 (13)

Table S6. Selected hydrogen-bond parameters for complex **3.**

D—H···*A*	*D*—H (Å)	H···*A* (Å)	*D*···*A* (Å)	*D*—H···*A* (°)
C10—H10A···O5^{i}	0.95	2.57	3.381 (5)	144.1
C11—H11A···O5^{i}	0.99	2.57	3.321 (5)	132.9
C11—H11B···O1	0.99	2.54	3.078 (5)	114.0
C32—H32A···O9	0.95	2.53	3.345 (6)	143.7
C34—H34A···O9	0.95	2.47	3.301 (5)	146.4
C35—H35B···O4	0.99	2.56	3.099 (5)	113.9
C50—H50A···O5^{ii}	0.98	2.57	3.431 (6)	146.7
C50—H50C···O6^{iii}	0.98	2.55	3.428 (6)	149.7

Symmetry code(s): (i) -*x*+2, -*y*+1, -*z*+1; (ii) -*x*+2, -*y*+1, -*z*+2; (iii) -*x*+3/2, *y*-1/2, -*z*+3/2.

Table S7. Absorption and emission spectral data for complexes **1- 3**.

Solvent	Compound	absorbance λ_{max} (nm) ($\varepsilon(M^{-1}cm^{-1})$)		emission λ_{em} (nm)
		ligand transition	MLCT	
Water	1	340 (15740)	472 (1930), 642 (1490)	398
	2	338 (16530)	472 (2130), 641 (1640)	398
	3	257 (28400) 329 (13680)	472 (1980), 641 (1540)	397
Buffer	1	343 (20370)	473 (1940), 642(1460)	398
	2	344 (20640)	471(2350), 639 (1700)	397
	3	344 (18790)	469 (2770), 639 (1840)	397
Ethanol	1	333 (22400)	477 (2100), 643 (1500)	389
	2	332 (24000)	477 (2100), 643 (1530)	389
	3	333 (20660) 250 (28040)	477 (2140), 643 (1570)	388
Acetonitrile	1	331 (22100)	479 (1630), 643 (1090)	385
	2	331 (23960) 290 (18990)	478 (1030), 643 (680)	384
	3	332 (22580)	480 (1970), 641 (1340)	387

DMF	1	333 (22130)	487 (2170), 644 (1360)	384
	2	333 (24080) 292 (19820)	485 (440), 645 (240)	384
	3	334 (22920) 289 (17670)	487 (1750), 643 (1090)	387

(a)

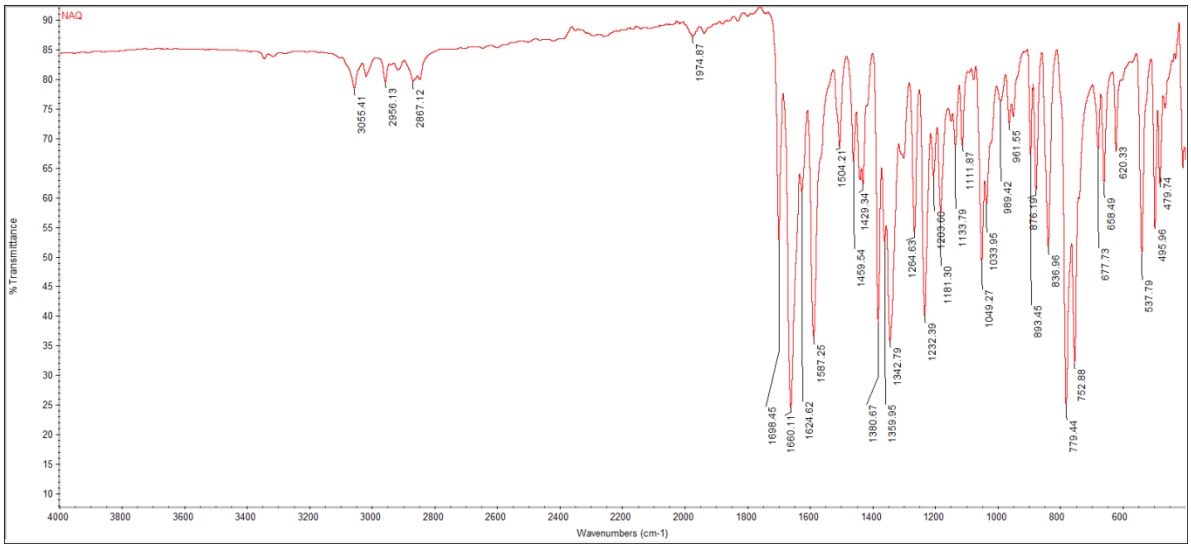

(b)

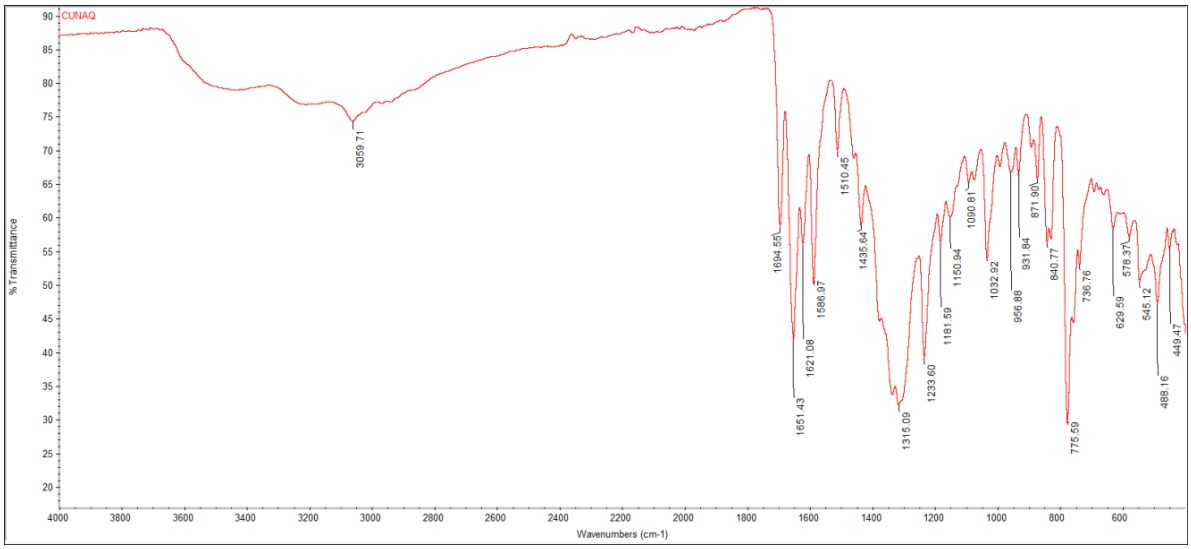

(c)

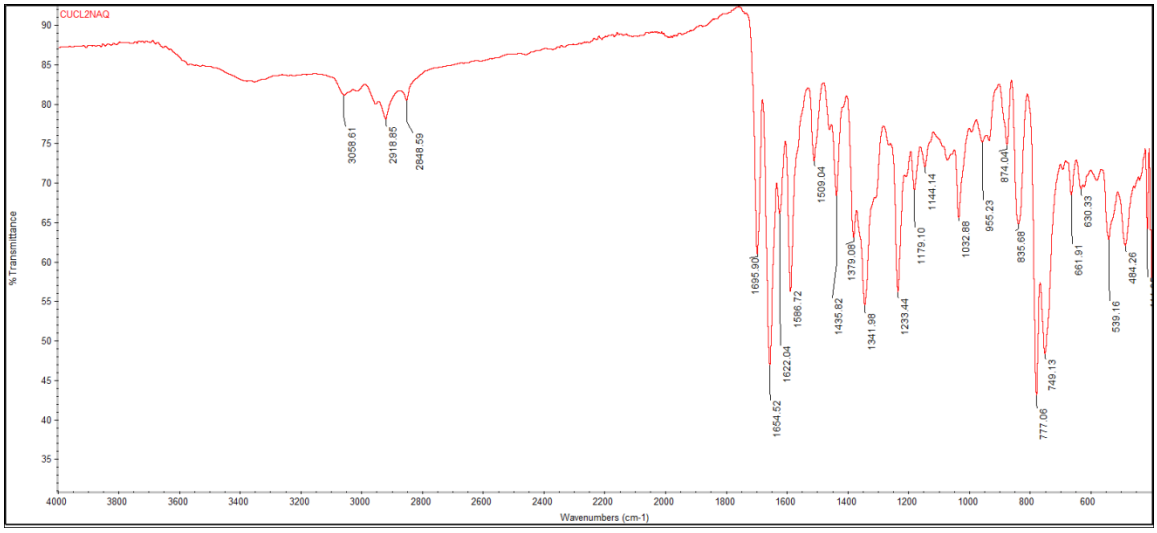

(d)

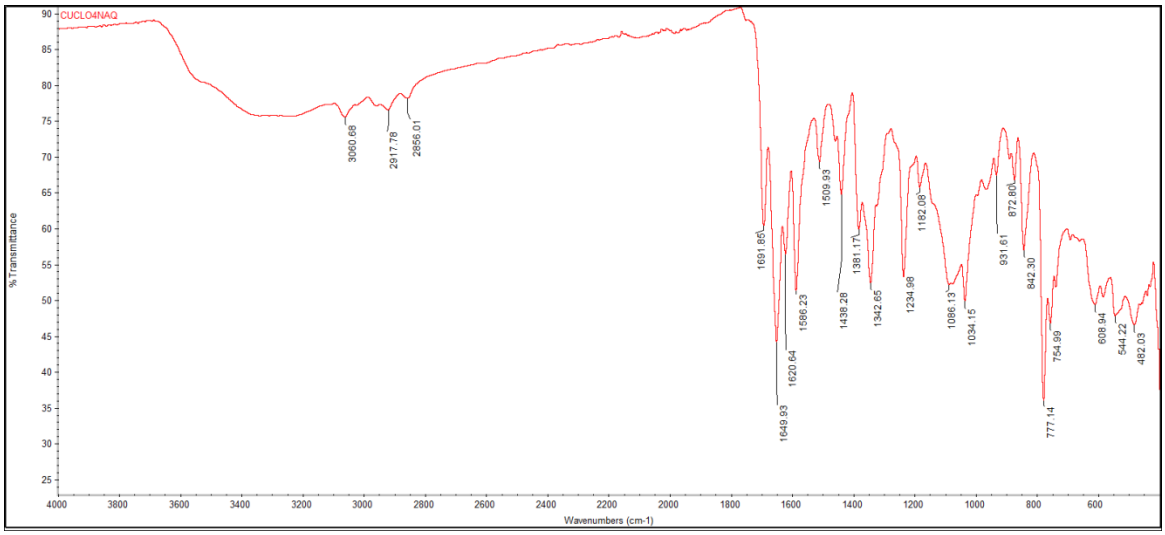

Figure S1. FT-IR spectra of (a) ligand (**L**), (b) **1**, (c) **2**, (d) **3**.

(a)

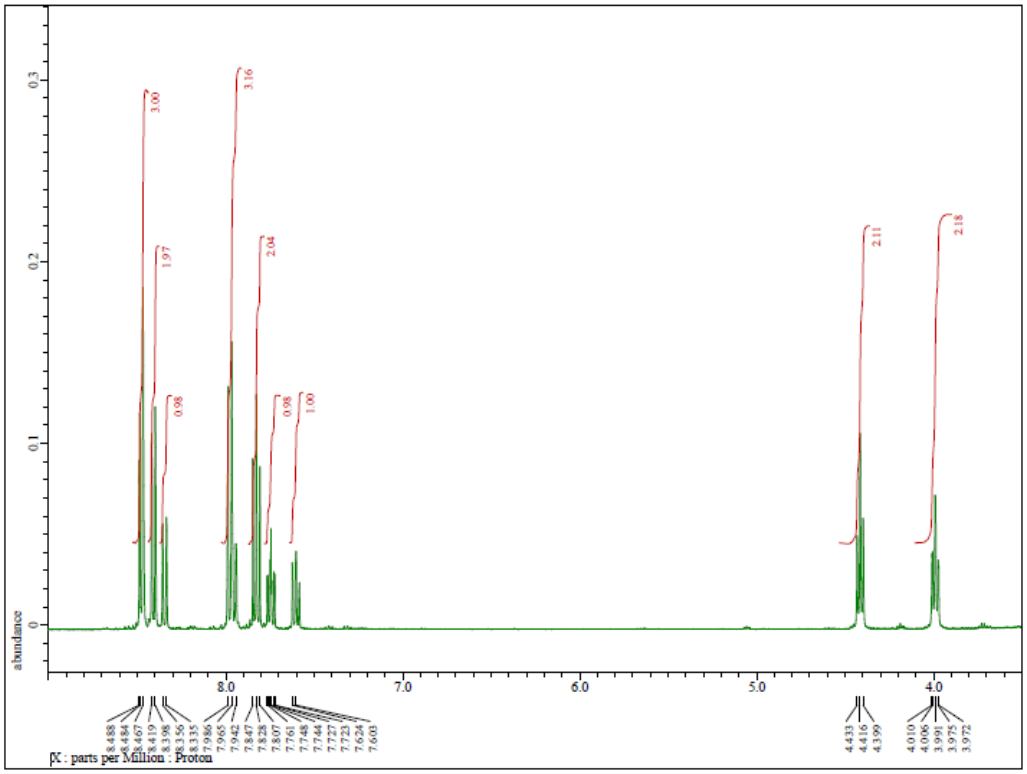

(b)

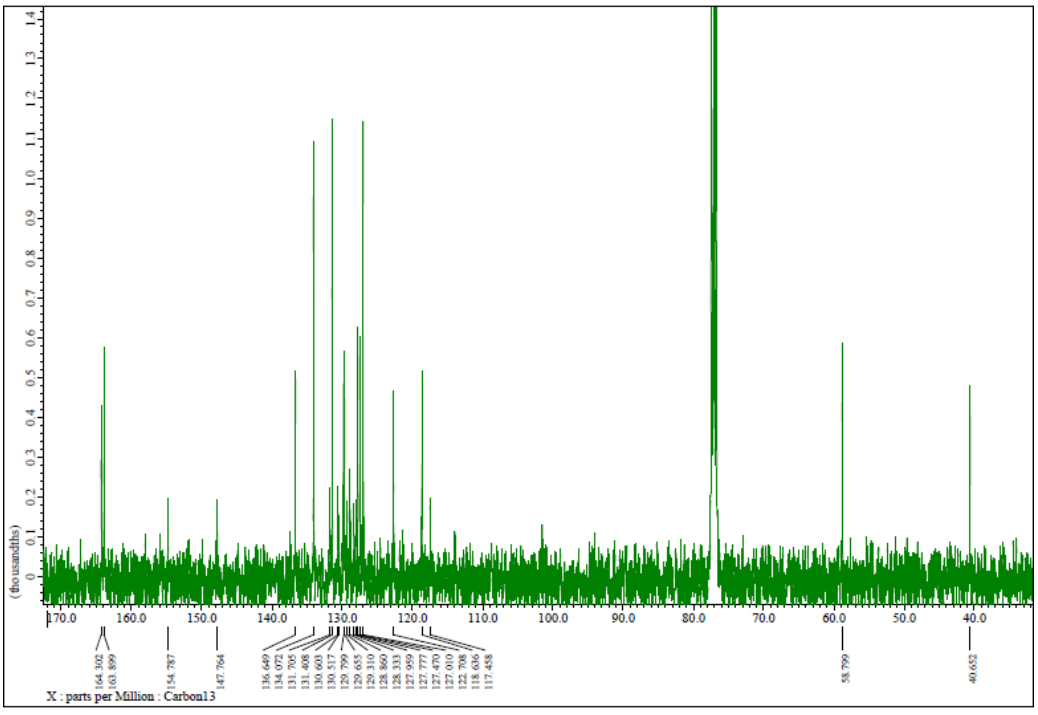

Figure S2. NMR spectra of ligand (**L**) (a) ^{1}H NMR, (b) ^{13}C NMR.

(a)

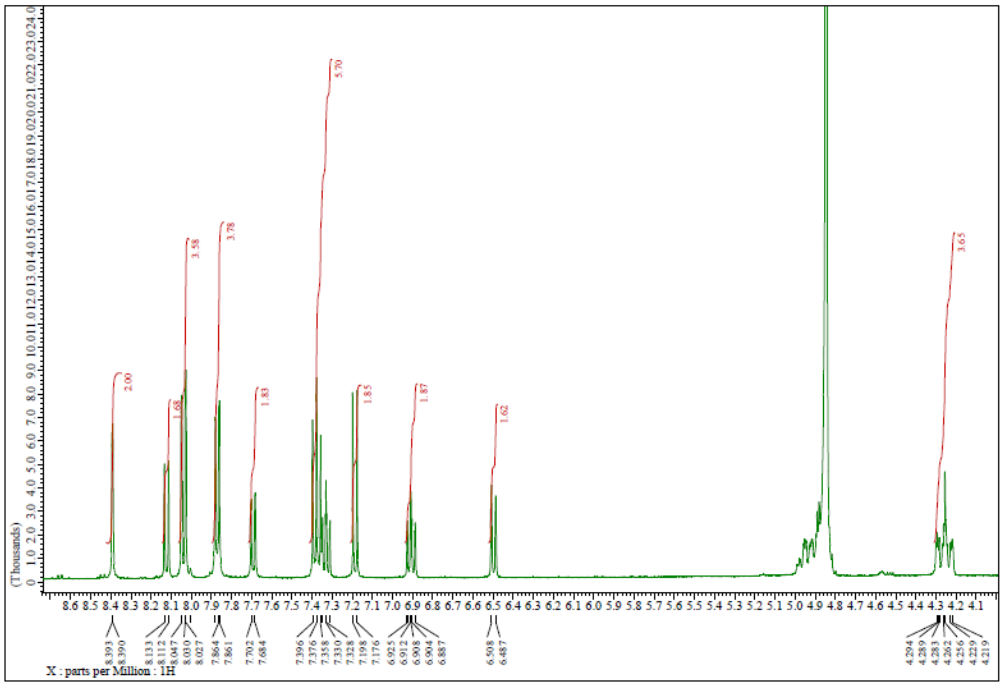

(b)

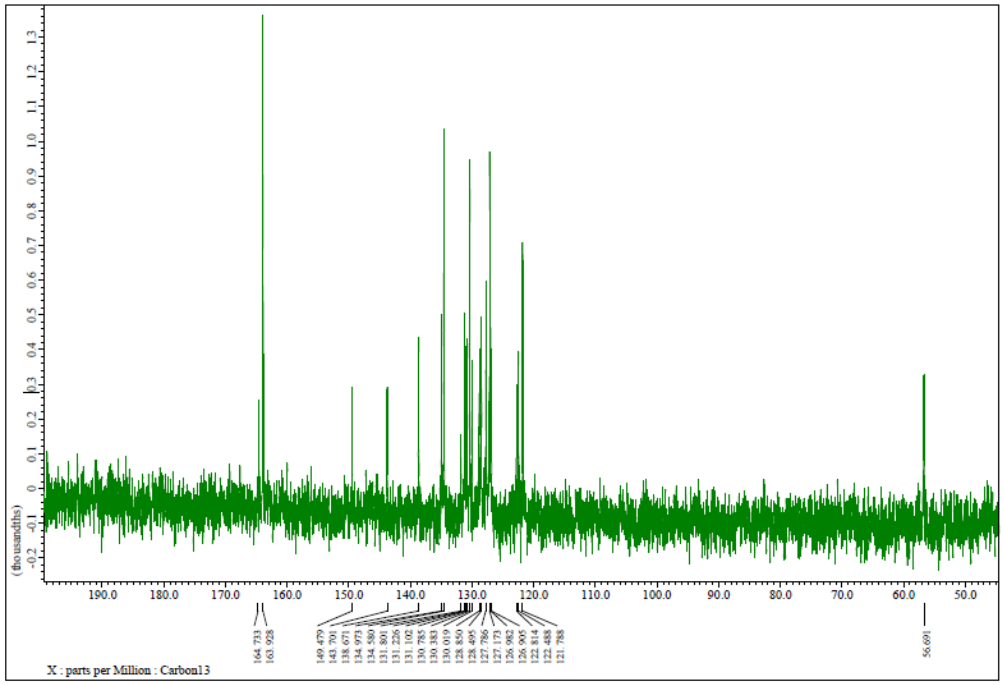

Figure S3. NMR spectra of complex **1** (a) ^{1}H NMR, (b) ^{13}C NMR.

(a)

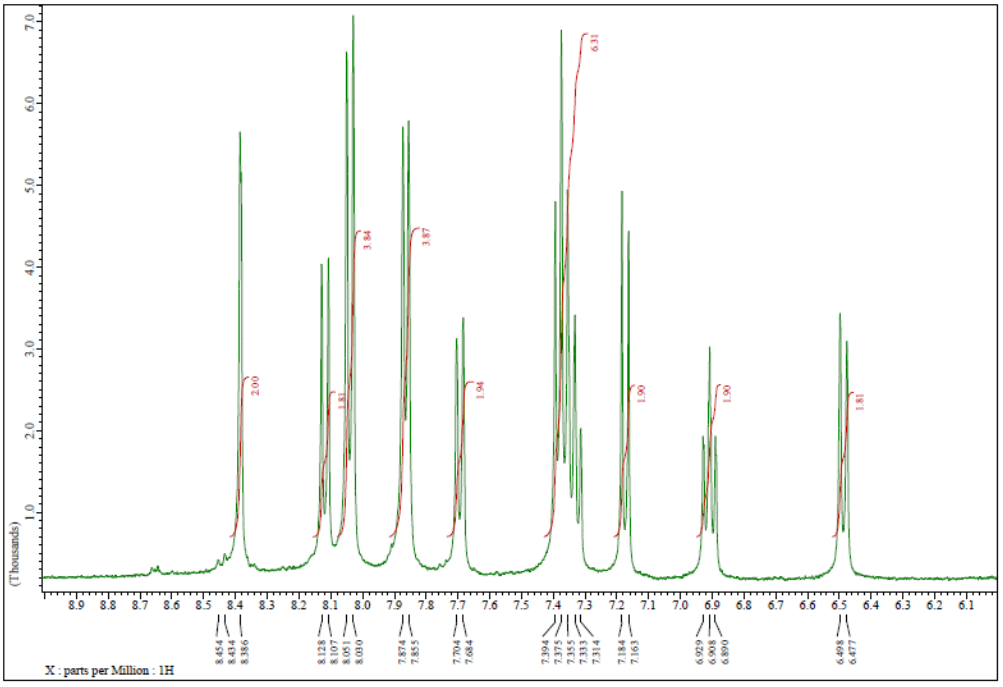

(b)

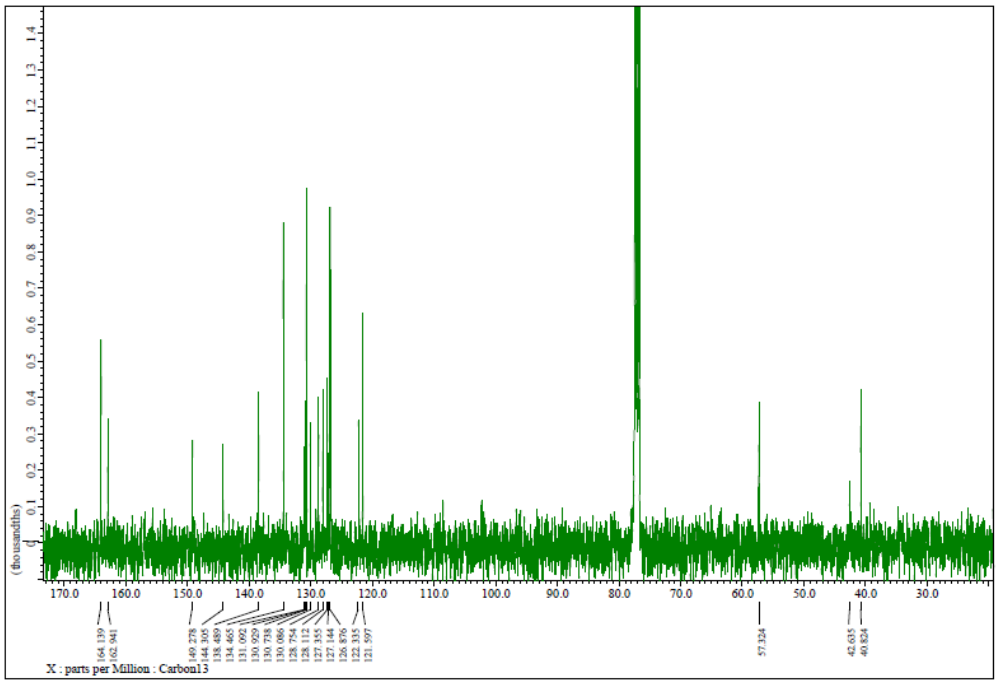

Figure S4. NMR spectra of complex **2** (a) ^{1}H NMR, (b) ^{13}C NMR.

(a)

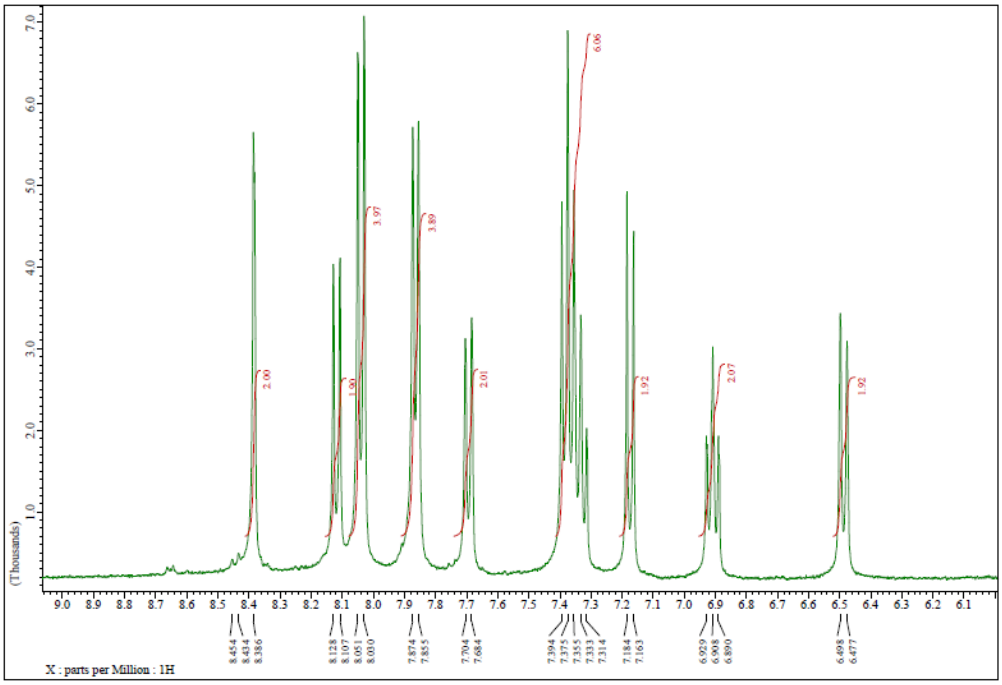

(b)

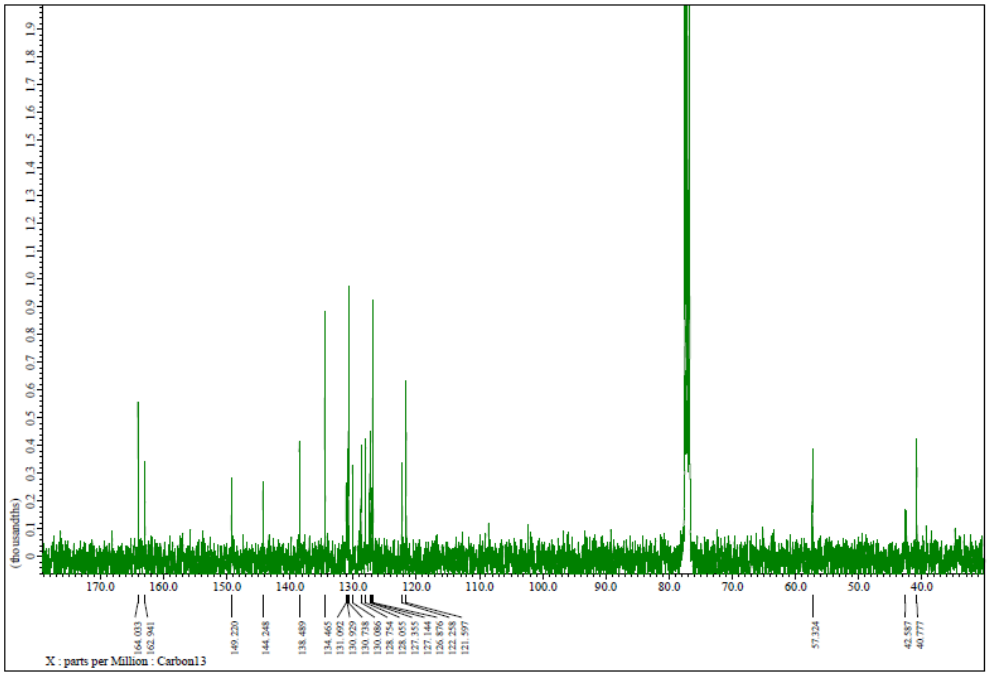

Figure S5. NMR spectra ofcomplex **3** (a) ^{1}H NMR, (b) ^{13}C NMR.

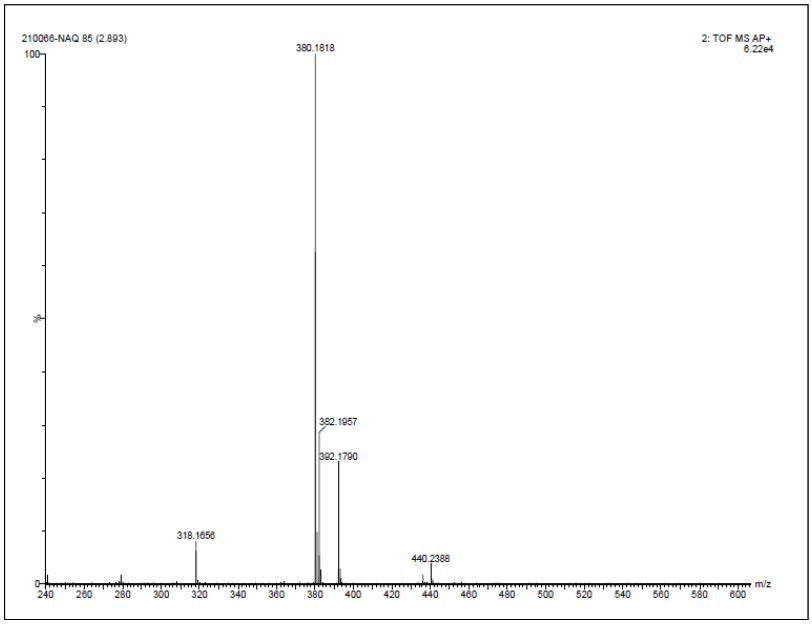

Figure S6. LC-MS spectrum of the ligand **L** showing significant peak at m/z 380 corresponds to [M+H].

(a)

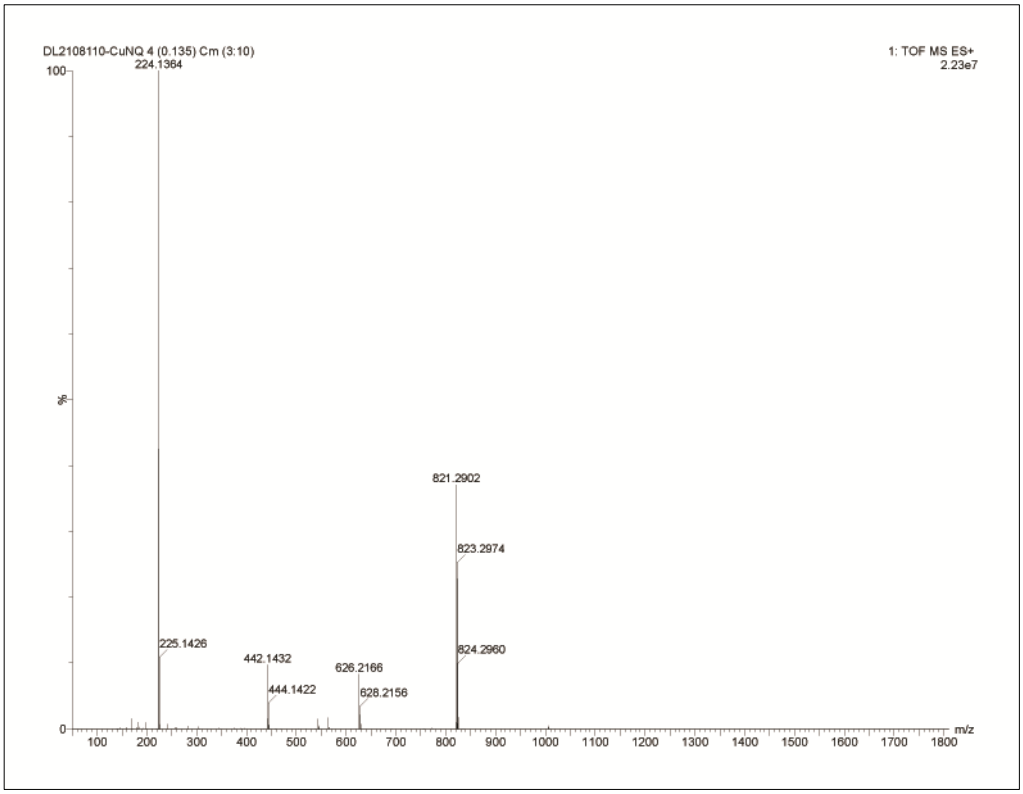

(b)

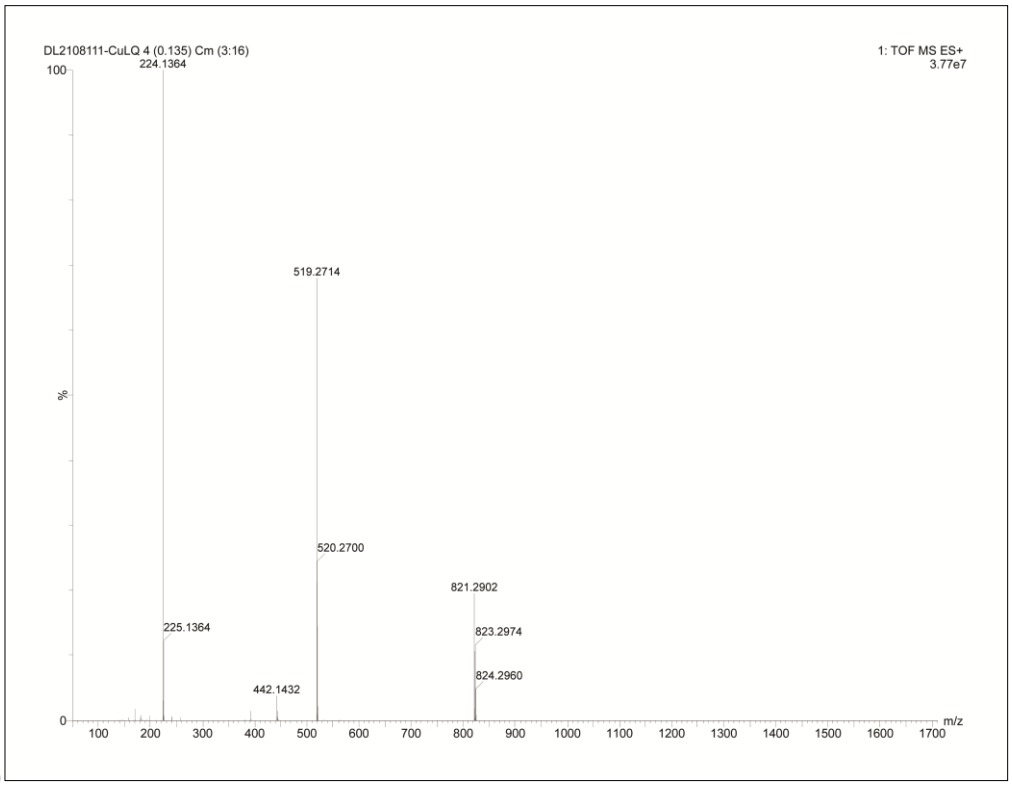

(c)

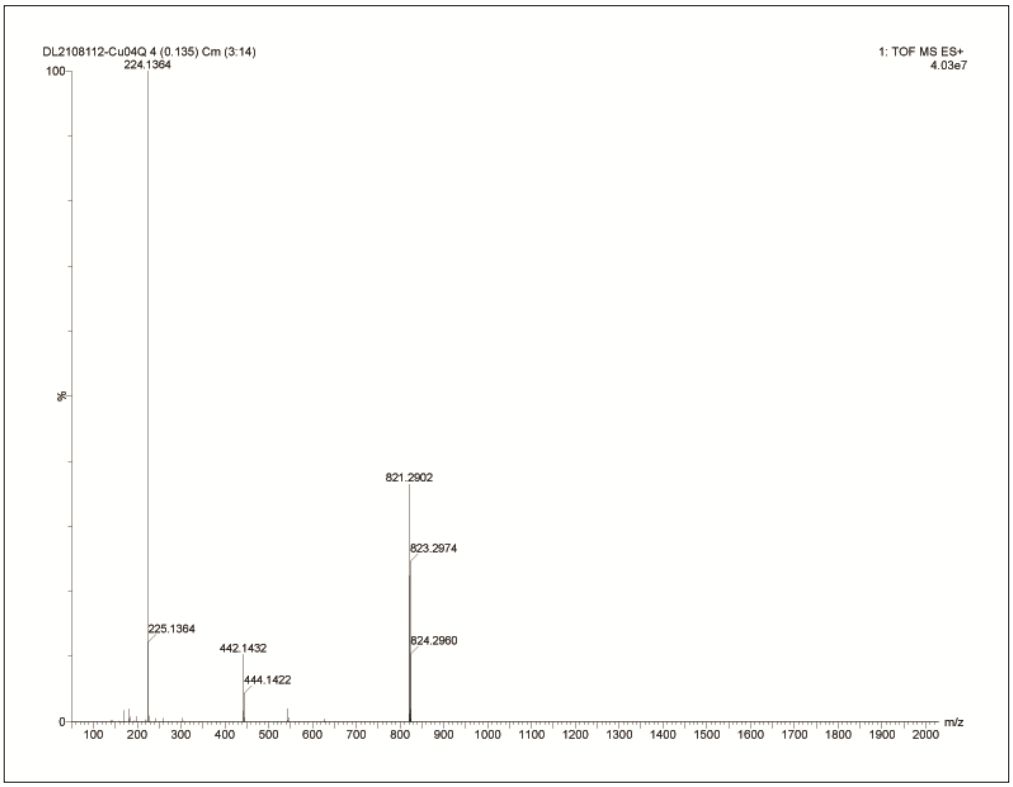

Figure S7. ESI-MS spectra of the complexes (a) **1**, (b) **2,** (c) **3**.

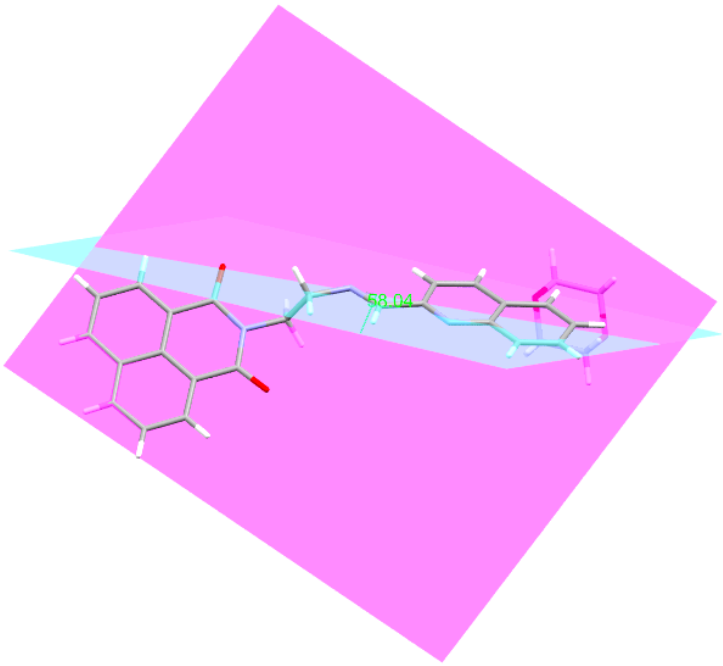

Figure S8. The ligand is not planar, the planes are intersecting at 82.42º.

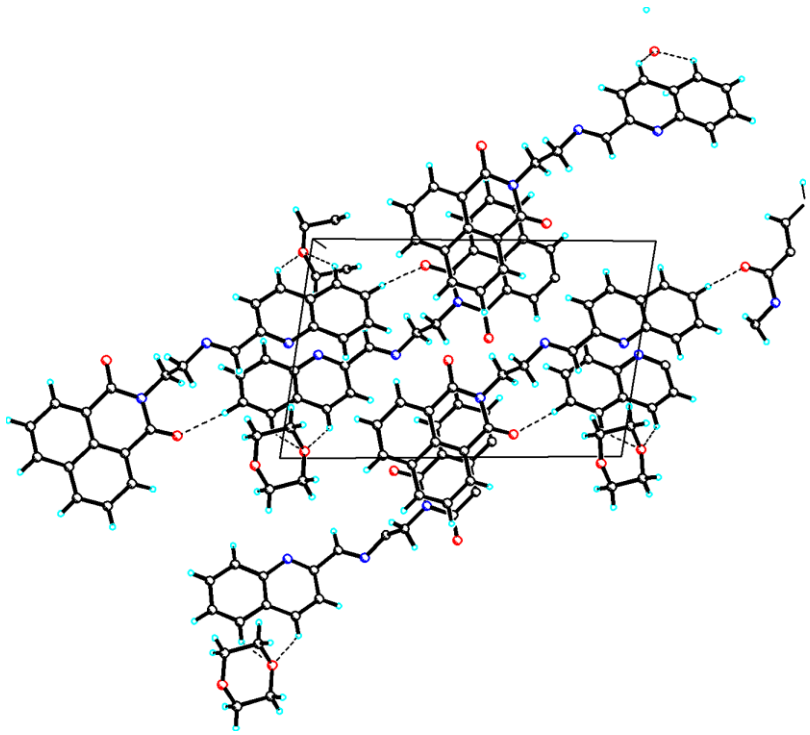

Figure S9. Packing diagram of ligand (**L**) showing intramolecular hydrogen bonding

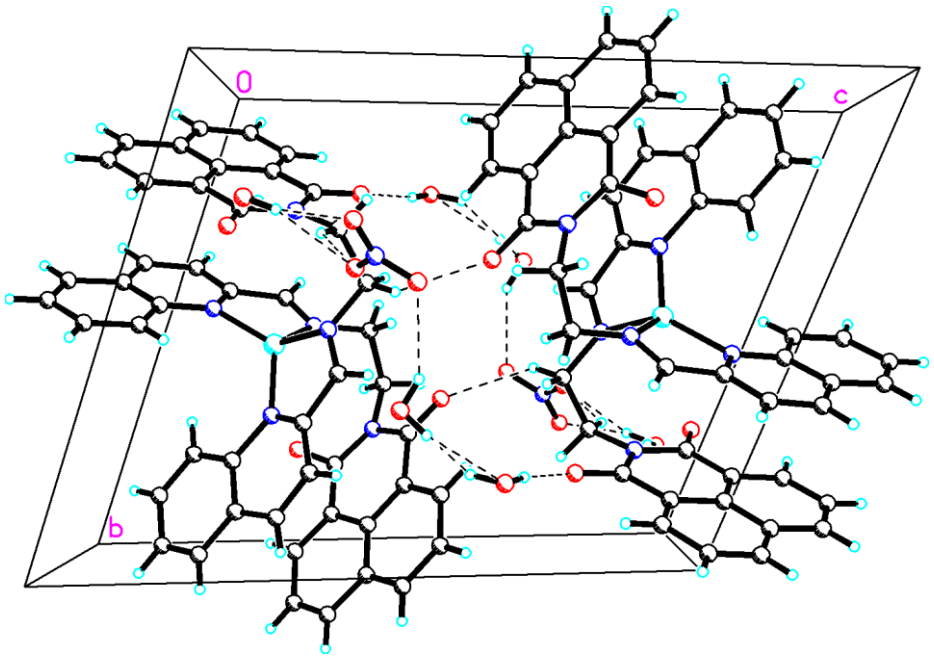

(a)

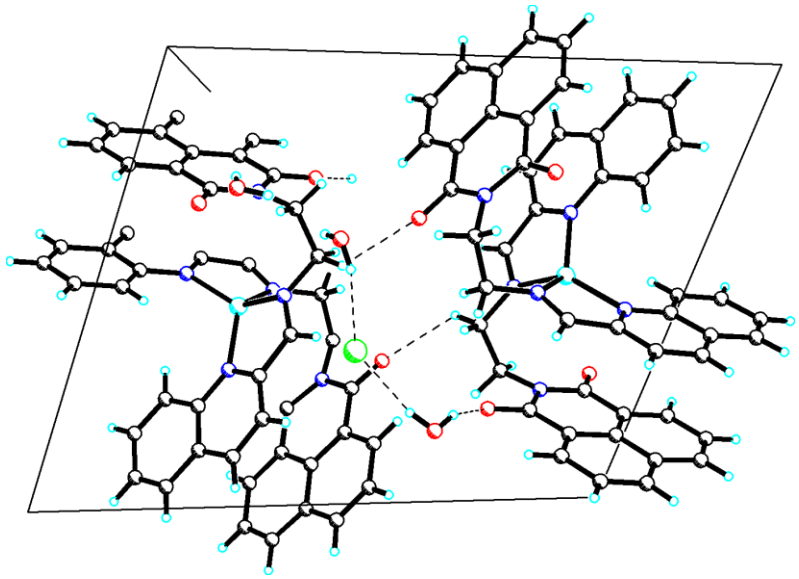

(b)

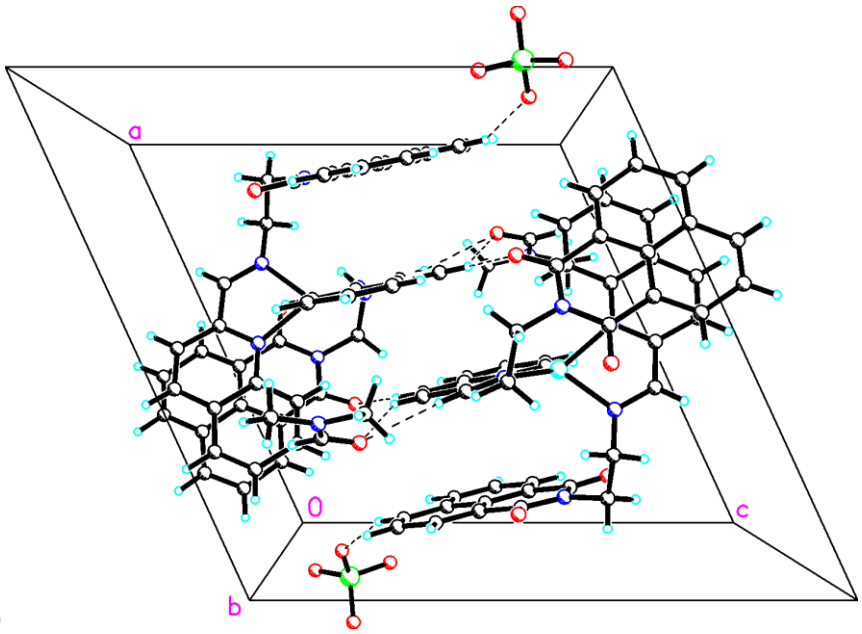

(c)

Figure S10. Packing diagram of complexes (a) **1**, (b) **2** and (c) **3** showing intermolecular hydrogen bonding.

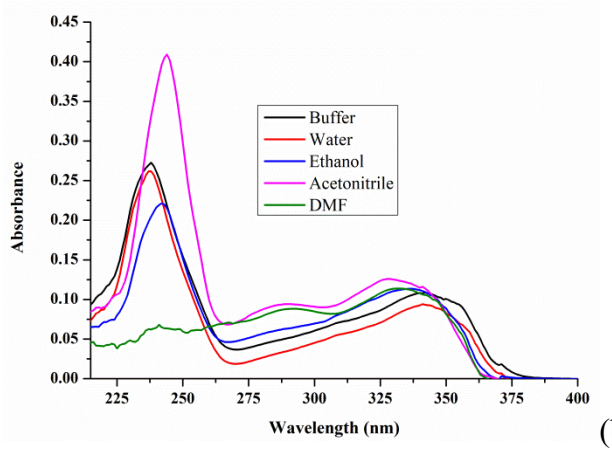

(a)

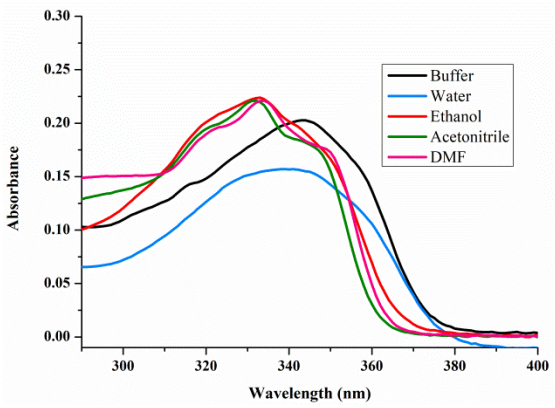

(b)

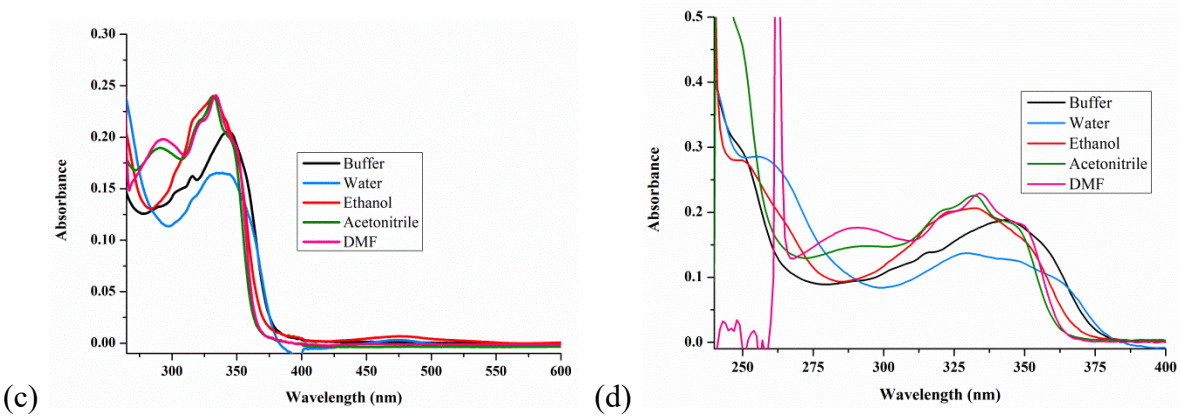

Figure S11. Absorption spectra for ligand (a) **L,** complexes (b) **1**, (c) **2**, (d) **3** (10 μM) in different solvents , buffer, water, ethanol, acetonitrile, DMF.

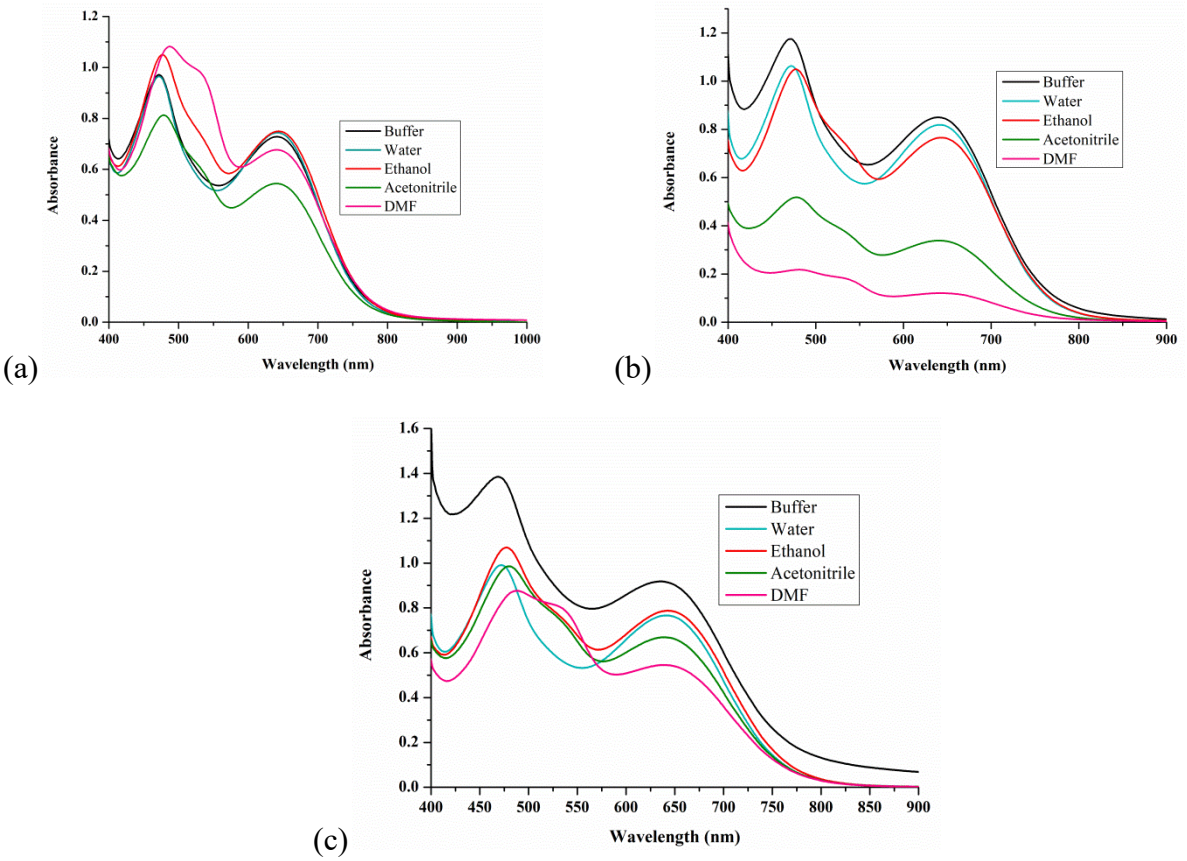

Figure S12. MLCT transition for complxes (a) **1,** (b) **2,** (c) **3** in various solvents buffer, water, ethanol, acetonitrile, DMF (0.5 mM).

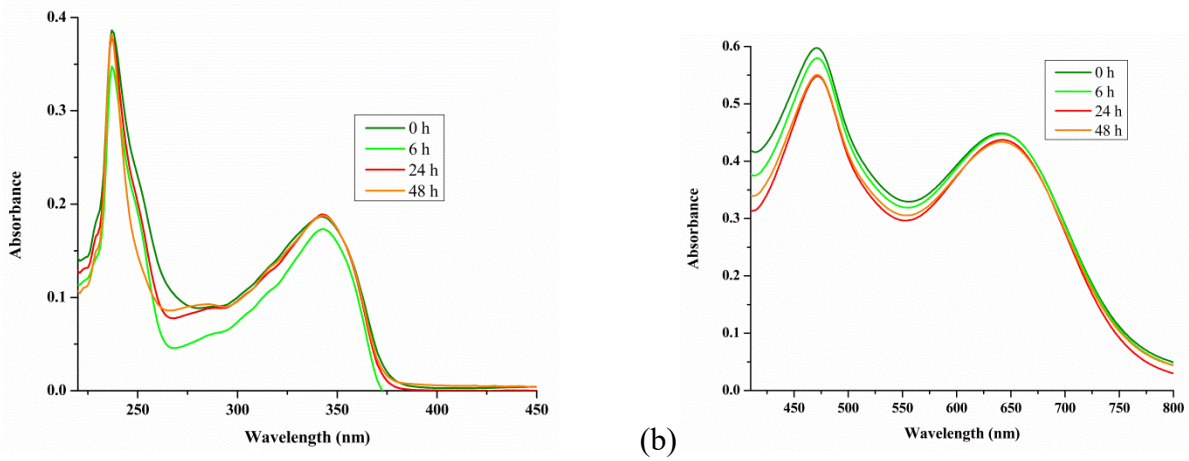

Figure S13. UV-vis spectra of complex **1** recorded at 0, 6, 24 and 48 h to check the stability of the complex.

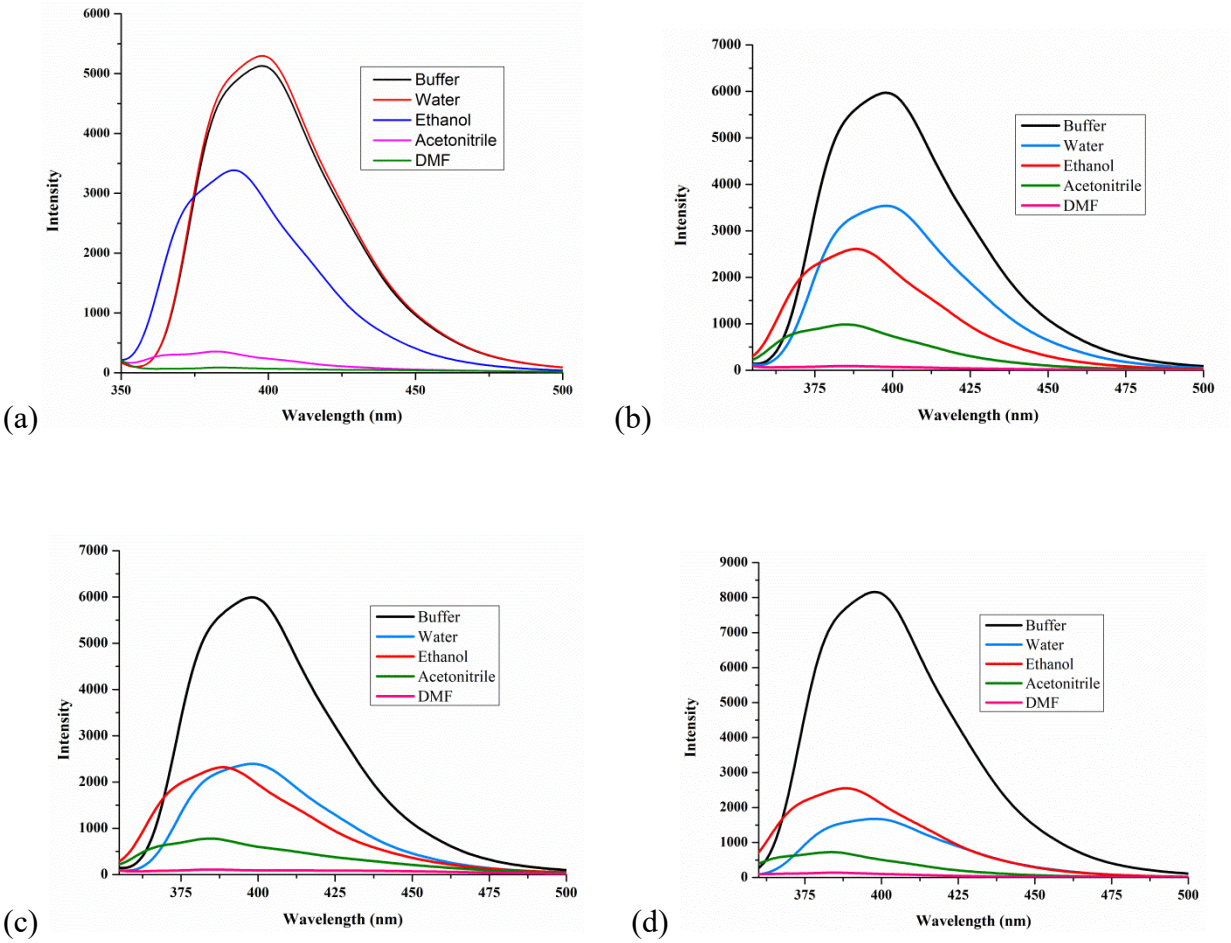

Figure S14. Emission spectra for complexes (a) **L** (b) **1**, (c) **2**, (d) **3** (10 μM) in different solvents, buffer, water, ethanol, acetonitrile, DMF excitation at 340 nm.

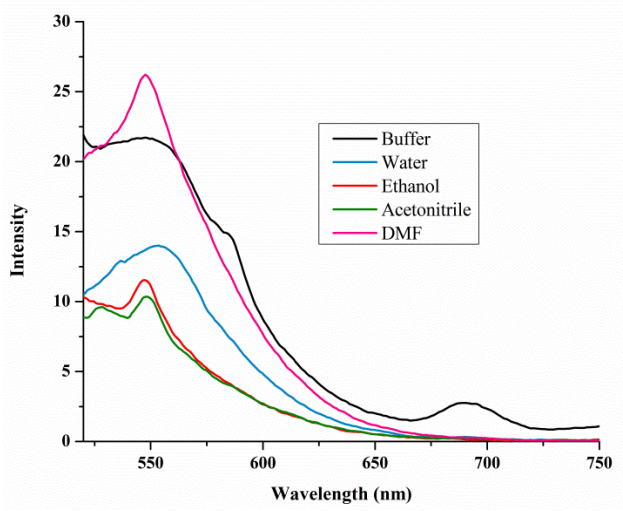

Figure S15. Emission spectra for complex **1** (100 μM) in different solvents, buffer, water, ethanol, acetonitrile, DMF excitation at 470 nm.

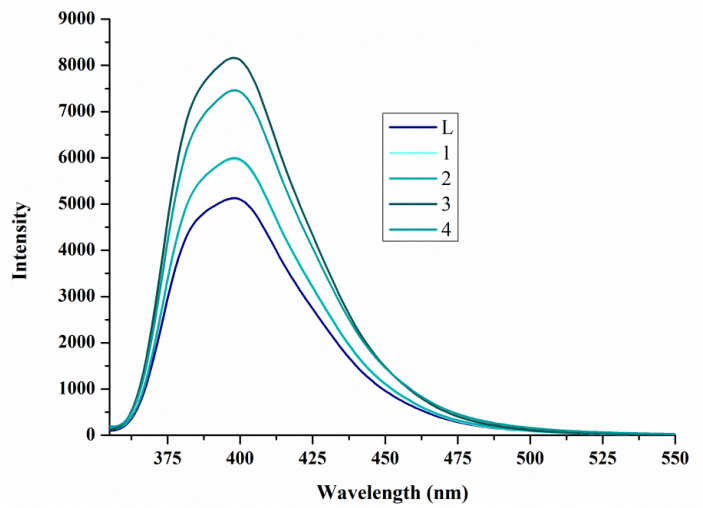

Figure S16. Complexes **1-3** show enhanced fluorescence intensity compared to ligand **L.**

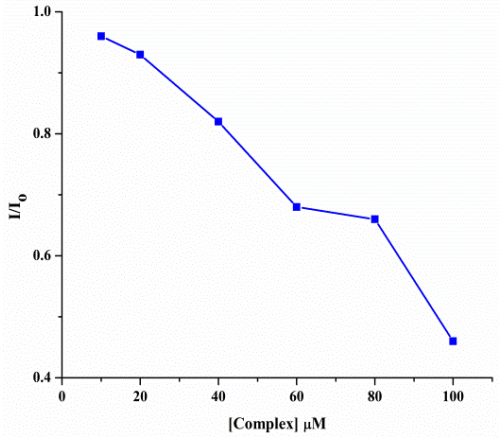

Figure 17 . Plot illustrating the relative integrated emission intensity versus [Cu] for the complex **1.**

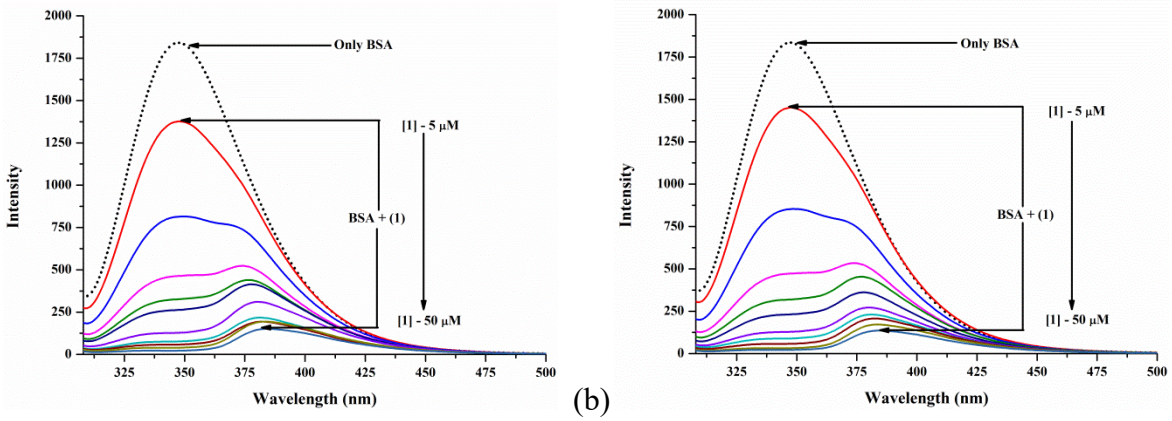

(a) (b)

Figure S18. Emission spectra for the interaction of BSA with complex **1**, Flourescence intensity decreases with the addition of increasing concentration of complex: 5, 10, 15, 20, 25, 30, 35, 40, 45 and 50 µM measured at (a) 306K and (b) 313K.

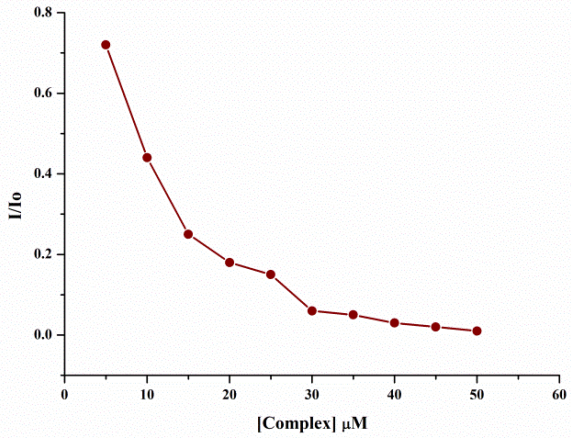

Figure 19. Plot illustrating the relative integrated emission intensity versus [Cu] for the complex **1**.

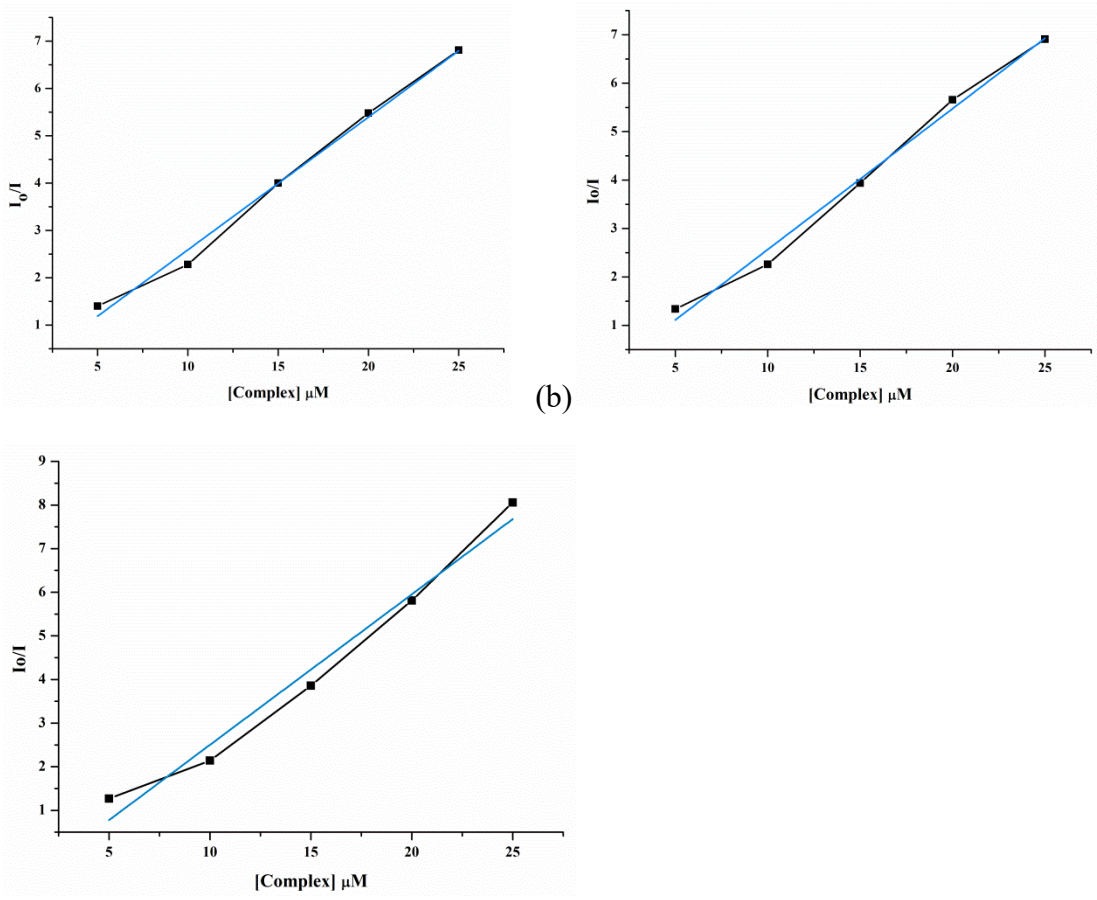

Figure S20. The Stern –Volmer graphs for the fluorescence quenching of BSA by complex **1** at (a) 301K, (b) 306K, (c) 313K.

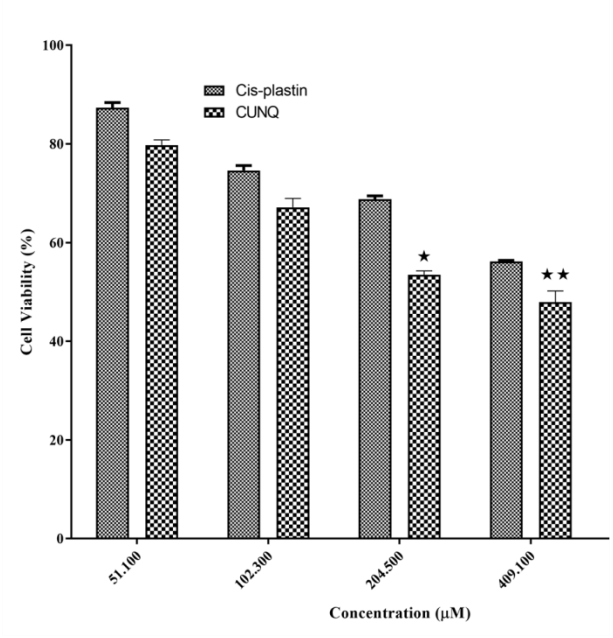

Figure S21. Cytotoxicity of complex **1** was measured with MTT assay for HEK cell lines in comparison with *cis*-platin.